

Nanoscale

Accepted Manuscript



This is an *Accepted Manuscript*, which has been through the Royal Society of Chemistry peer review process and has been accepted for publication.

Accepted Manuscripts are published online shortly after acceptance, before technical editing, formatting and proof reading. Using this free service, authors can make their results available to the community, in citable form, before we publish the edited article. We will replace this *Accepted Manuscript* with the edited and formatted *Advance Article* as soon as it is available.

You can find more information about *Accepted Manuscripts* in the [Information for Authors](#).

Please note that technical editing may introduce minor changes to the text and/or graphics, which may alter content. The journal's standard [Terms & Conditions](#) and the [Ethical guidelines](#) still apply. In no event shall the Royal Society of Chemistry be held responsible for any errors or omissions in this *Accepted Manuscript* or any consequences arising from the use of any information it contains.

ARTICLE

Bonding and electronic states of boron in silicon nanowires characterized by infrared synchrotron radiation beam

Cite this: DOI: 10.1039/x0xx00000x

N. Fukata,^{*a} W. Jevasuwan,^a Y. Ikemoto^b and T. Moriwaki^b,Received 00th January 2012,
Accepted 00th January 2012

DOI: 10.1039/x0xx00000x

www.rsc.org/

The infrared synchrotron radiation (IR-SR) beamline of SPring-8 as an IR light source was applied to characterize boron (B) atoms in silicon nanowires (SiNWs). The use of an IR-SR beam with much higher brilliance than conventional IR light sources and a wide range of wavenumbers from visible to far IR regions made it possible to detect a local vibrational mode of B in SiNWs. Use of this technique also made it possible to detect other IR peaks related to transitions of a bound hole from the ground state of a B acceptor atom to excited states, clarifying the electronic state of B acceptors in SiNWs.

1. Introduction

The novel physical properties of silicon nanowires (SiNWs) make them of great interest in the fields of both fundamental and applied research. Numerous research results demonstrate their potential for future application to electronic devices and solar cells.¹⁻⁴ However, to be able to realize nanoscale silicon devices and solar cells using SiNWs, it is important to first investigate impurity doping mechanisms. Various results concerning electrical transport in phosphorus (P)- or boron (B)-doped SiNWs have thus far been reported.⁵⁻⁹ Impurity doping will be of increasing importance in realizing core-shell NWs using Si and Ge for high-speed transistor channels.¹⁰⁻¹⁴ To be able to clarify the states of impurity atoms, such as their chemical bonding states and electrical activity, we applied Raman scattering and electron spin resonance (ESR).¹⁵⁻¹⁸ Local vibrational modes of ¹¹B and ¹⁰B in SiNWs were observed by Raman scattering measurements, indicating B doping into the crystalline Si core of SiNWs. Asymmetric broadening due to Fano resonance was also observed in the Si optical phonon peak, showing the electrical activity of B atoms in SiNWs. These techniques also clarified the segregation behaviours of B and P atoms in SiNWs.¹⁹ Fourier-transform infrared (FT-IR) techniques also allow the vibrational characterization of impurity atoms in bulk Si. However, it is very difficult to apply FT-IR techniques to characterize impurity atoms in nanostructures due to the difficulty of preparing sufficiently large samples. Use of IR synchrotron radiation (IR-SR) as an IR light source has the advantages of a greater brilliance than conventional IR light sources using thermal radiation and a wide range of wavenumbers, from the visible to far IR regions, making it possible to characterize nanostructures materials such as SiNWs. The details of properties and advantages of the micro-FT-IR using IR-SR are shown in the supporting information.

The passivation of B by hydrogen (H) has been extensively studied in B-doped bulk Si.²⁰⁻²⁵ The H atoms migrate to the bond-centered (BC) sites between B and neighboring host Si atoms, forming what are termed H-B passivation centers, resulting in the passivation of B acceptor atoms. The H passivation of B in SiNWs can be investigated by the observation of B local vibration in H-B passivation centers perturbed by H.

In this study, we carried out B doping during the growth of SiNWs and investigated the states of B atoms in SiNWs and their hydrogen passivation effect by means of micro-FT-IR measurements at 4.2 K, using the IR synchrotron radiation (IR-SR) beamline (BL43IR) at SPring-8 in Japan. We also used micro-Raman scattering measurements to identify the IR peaks.

2. Experimental details

SiNWs were synthesized by laser ablation of an Si target with nickel (Ni) as the metal catalyst. B atoms were also included in the target as dopant impurities. Three kinds of targets, namely Si₈₉Ni₁B₁₀, Si₉₈Ni₁B₁, and Si₉₉Ni₁, were used to grow SiNWs. The growth mechanism of SiNWs is VLS (vapor-liquid-solid) growth.²⁶ The targets were placed in a quartz tube heated to 1200 °C in a flow of Ar gas (50 sccm) and of H₂ gas (10 sccm). A frequency-doubled NdYAG laser (532 nm, 150 - 180 mJ/pulse) was used to ablate these targets. SiNWs were grown in an Ar gas atmosphere and then deposited on n-type Si substrates with a high-resistivity of 1-50 Ωcm.

Scanning transmission electron microscopy (STEM) and transmission electron microscopy (TEM) were used to investigate the detailed structures. Micro-FTIR measurements were conducted using the IR-SR beamline at SPring-8. A schematic illustration is shown in Fig. 1. The focus size of the IR-SR is 10 times smaller, and the light density 10² times higher, than black body light, and this allowed the optical

spectrum in even microscopic regions to be measured up to lower frequency regions through a window of cryostat. The IR-SR absorption peaks were observed at 4.2 K using a continuous-flow liquid-helium cryostat with KRS-5 windows. The spectral resolution was about 2 cm^{-1} . Micro-Raman scattering measurements were performed at room temperature (RT) with a 100x objective and excitation light at 532 nm. The excitation power was set at about 0.02 mW to prevent local heating effects from the excitation laser.^{27,28} The spectral resolution was about 0.2 cm^{-1} . Hydrogen atom treatment (HAT) using remote downstream methods of high-flux H atoms was performed at 180 °C for 30 min. This is the most appropriate temperature for the passivation of B in Si. With this method, the specimens were placed in a quartz tube at a distance of 60 cm from the plasma source and hydrogenated only with H atoms. Damage by H plasma was thus completely prevented. The details of the laser ablation and hydrogenation procedures are reported in Refs [28] and [29].

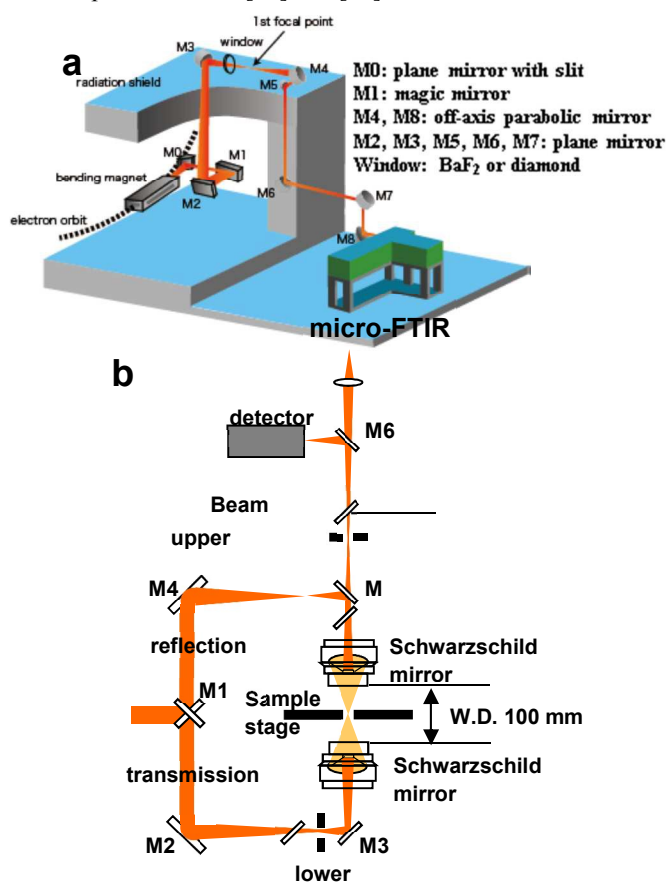


Fig. 1 Schematic illustrations of (a) a micro-FTIR system using the IR synchrotron radiation (IR-SR) beamline at SPring-8 and (b) the optics in the infrared microscope. (b) Each M denotes a mirror.

3. Results and discussion

Fig. 2a is a schematic illustration of our laser ablation system for the synthesis of SiNWs. A special collector made of quartz was installed in the quartz tube to effectively collect SiNWs grown in an Ar gas atmosphere (Fig. 2a and 2b). Laser ablation was continued for 3 hours to deposit thick layers of SiNWs with the aim of increasing the optical absorption by B atoms.

The thickness of the layer of SiNWs reached several tens of micrometers (Fig. 2d). Typical STEM and high-resolution TEM images of SiNWs synthesized using Si₉₈Ni₁B₁ targets (Fig. 2c) are shown in Fig. 2e and 2f. The SiNWs are composed of a crystalline Si core and surface oxide layer. The average core diameter was about 20 nm and the thickness of the surface oxide layer was about 10 nm.

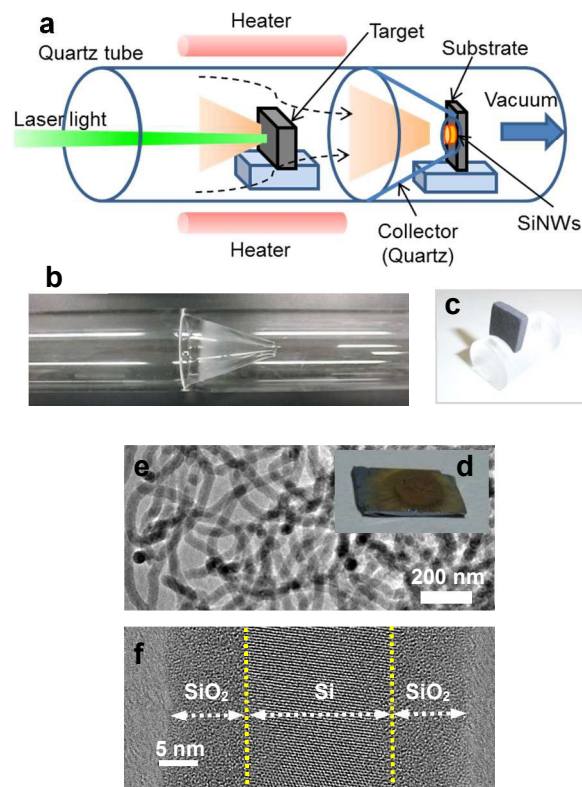


Fig. 2 (a) Schematic illustration of synthesis of SiNWs by a laser ablation system. Photographs of (b) a quartz tube with a collector, (c) a target and (d) a sample for IR synchrotron radiation measurements. Typical (e) STEM and (f) high-resolution TEM images of SiNWs synthesized using the Si₉₈Ni₁B₁₀ target.

Fig. 3 shows whole range of IR-SR absorption spectra observed for B-doped and undoped SiNWs. Four peaks were observed at 468, 806, 1085, and 1200 cm^{-1} for both samples, and assigned to different oxygen-related modes in the surface oxide layer of SiNWs by comparison with the results for bulk silicon.³⁰ The first peak, at 468 cm^{-1} , is due to the rocking mode of the O atom about the axis through the two Si atoms. The second peak, at 806 cm^{-1} , is due to symmetrical stretching of the O atom along the line bisecting the axis formed by the two Si atoms. The third and fourth peaks, at 1085 and 1200 cm^{-1} , are due to the asymmetrical stretching motion of the O atoms. In this stretching motion, the O atoms move back and forth along a line parallel to the axis through the two Si atoms. These results show that our IR-SR technique is applicable even for the characterization of Si nanostructures. In addition to these oxygen-related peaks, a new peak was observed at about 625 cm^{-1} in B-doped SiNWs.

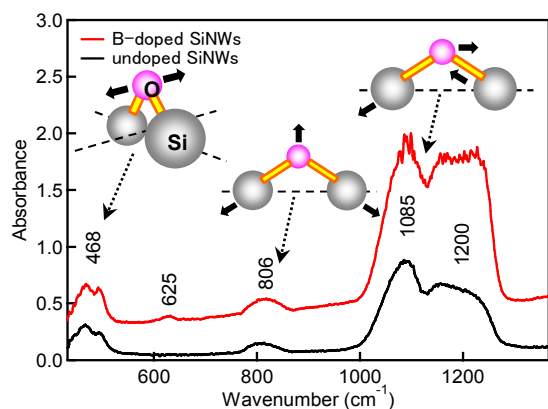


Fig. 3 IR-SR absorption spectra observed for B-doped and undoped SiNWs. B-doped SiNWs were synthesized using $\text{Si}_{98}\text{Ni}_1\text{B}_1$ targets.

The dependence of the B concentration is shown in Fig. 4a and 4c: the peak intensity increases on increasing the B concentration. The peak position is similar to the Raman result (618 cm^{-1}) shown in Fig. 4b. The Raman peaks at about 618 and 643 cm^{-1} have been assigned to ^{11}B and ^{10}B local

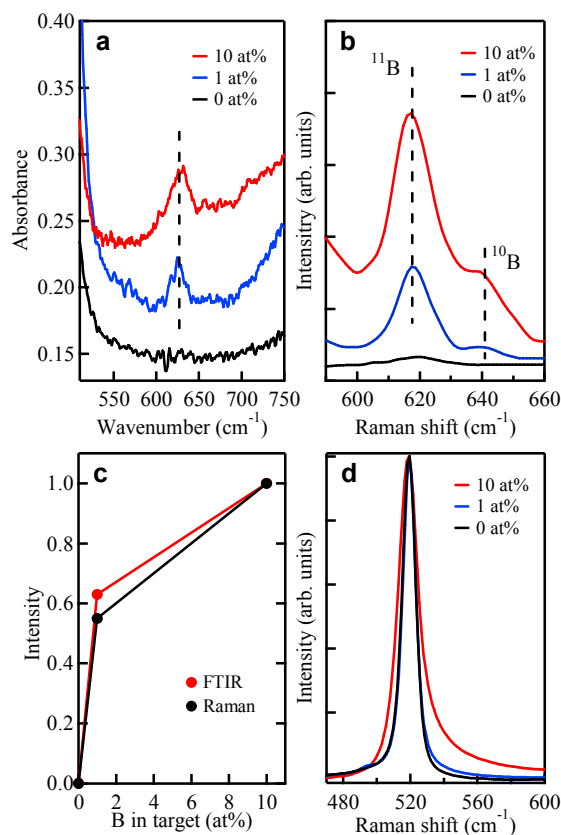


Fig. 4 (a) IR-SR absorption spectra and (b) Raman spectra observed for B-doped and undoped SiNWs. (c) Dependence of the peak intensity of the IR-SR absorption peak at 625 cm^{-1} and ^{11}B local vibrational peak on the content of B in the ablated targets. (d) Si optical phonon peaks observed for B-doped and undoped SiNWs by Raman scattering measurements.

vibrational peaks in B-doped SiNWs.^{15,17} The peak assignments were made based on the notion that the peak frequencies are in good agreement with those of the local vibrational modes of B in bulk Si crystal.³¹ The peak shift can be fully explained by the isotope shift of B atoms, and the ratio of the peak intensity is in good agreement with the natural abundance of B isotopes.^{15,17} The positions of the IR-SR absorption peaks are at higher frequencies than those of the Raman peaks. The Raman measurements were made at room temperature, while the IR-SR measurements were made at 4.2 K . Hence, the higher frequency shift at lower temperatures can be explained mainly by the temperature effect. The ^{10}B local vibrational mode should be observed at around 650 cm^{-1} , but was not clearly apparent due to the low signal intensity and the high background signal. The intensity of the IR-SR peak at 625 cm^{-1} shows a good correlation with that of the Raman result in Fig. 4c. Based on the peak position and its dependence on the B doping level, the newly observed IR-SR peak at 625 cm^{-1} is assigned to the B vibrational peak in SiNWs. The Si optical phonon peak was also observed by the Raman scattering measurements shown in Fig. 4d. The phonon peak showed asymmetric broadening to a higher wavenumber due to the Fano effect, showing that B atoms are electrically activated in SiNWs. We analyzed the Si optical phonon peaks using the Fano equation and estimated the electrical active B concentration to be about 10^{19} and 10^{18} cm^{-3} for B-doped SiNWs using $\text{Si}_{89}\text{Ni}_1\text{B}_{10}$ and $\text{Si}_{98}\text{Ni}_1\text{B}_1$ targets, respectively. The proof of the Fano effect is shown in the supporting information.

To further verify B doping in SiNWs by IR-SR measurements, we investigated another frequency region where electronic transition of B in Si should be observed. The results are shown in Fig. 5. Two peaks were newly observed, at about 278 and 319 cm^{-1} . The high noise in the low-frequency region is due to the sensitivity of our IR-SR measurements. Burstein et al., while making low-temperature IR measurements of B-doped bulk silicon, were the first to note discrete electronic transitions of bound holes from the ground state of neutral B acceptor atoms to a series of hydrogen-like excited levels lying below the band edge.³² Other groups later reported similar

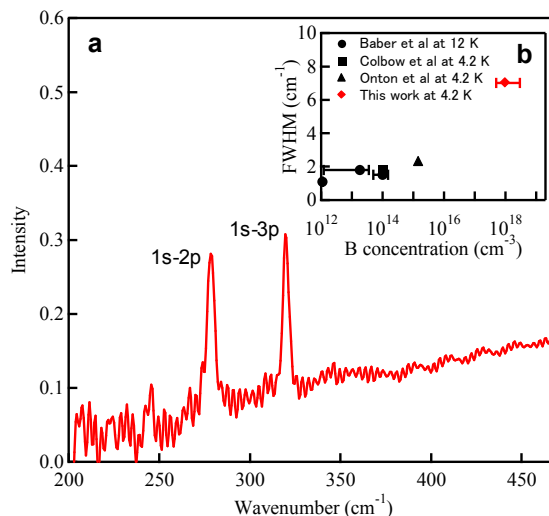


Fig. 5 (a) IR-SR absorption spectra related to electronic transition of B in SiNWs synthesized using $\text{Si}_{98}\text{Ni}_1\text{B}_1$ targets. (b) Dependence of FWHM on B concentration.

observations.^{33–36} The most characteristic peaks are observed at about 278 and 320 cm^{-1} and are respectively assigned to the 1s-2p and 1s-3p transitions of B in Si. The newly-observed peak positions for B-doped SiNWs correspond very closely to 1s-2p and 1s-3p transitions. These peaks were not observed for undoped SiNWs, showing that they are related to electronic transitions from the ground state of a neutral B acceptor atom to excited levels. The data for full width at half maximum of 1s-3p transition of B in SiNWs is plotted in Fig. 5b in addition to the previously reported data. The broadening of the absorption peaks is likely to be due to the effect of higher B doping in SiNWs.³⁴

The characterization of impurity atoms in SiNWs is often difficult, due to the sensitivity of the characterization methods and the measurement conditions. In particular, it is almost impossible to characterize single SiNW by FT-IR at the present time and therefore we prepared special samples as shown in Fig. 2d. The electronic transition peaks are difficult to observe in highly-doped samples in bulk Si, unlike in the case of local vibrational modes, and generally Si samples doped at less than 10^{15} cm^{-3} are used, since IR light cannot penetrate the samples due to strong absorption. The net sample thickness for B-doped SiNWs is very thin, at several tens of micrometers. The use of thinned samples, combined with a high-brilliance IR-SR beam, made it possible to evaluate the electronic transition of neutral B acceptor atoms in highly B-doped NW samples. This is the first observation of the electronic transition of neutral B acceptor atoms for highly B-doped Si materials. On the other hand, we also tried to make crystalline doped Si films with similar thickness by ion implantation for purpose of comparison. However, it was difficult to confine high concentration of B atoms in initial shallow regions even after activation annealing because B atoms easily diffuse to deeper regions by so called transient enhanced diffusion.³⁷

Impurity levels in nanostructures are known to become deep.³⁸ Our result for B-doped SiNWs with a diameter of 20 nm shows no significant change in impurity levels. It appears that thinner NWs are needed to observe impurity level shifts. A theoretical calculation of zero-dimensional Si nanocrystals doped with P showed that P is not a shallow donor in Si if the nanocrystals are less than 20 nm in diameter.³⁸ For one-dimensional SiNWs, a much smaller diameter is needed for the impurity level shift³⁹ because carriers are not confined along the growth direction of SiNWs. To investigate the impurity level shift for SiNWs with low diameters of less than 20 nm, we applied thermal oxidation after the growth of B-doped SiNWs. Thermal oxidation increases the thickness of the oxide layer, resulting in a decrease in the crystalline Si core diameter. It is also known that the thicker oxide shell has an influence on the position of the impurity energetic level into the gap.⁴⁰ The deepening of the impurity level into nanostructures is considered to be a direct consequence of the dielectric mismatch between the crystalline Si core of SiNWs and their surrounding oxide layers. Hence the impurity level shift can be also expected by the enhancement of the dielectric mismatch after thermal oxidation. The Si core diameter shrank by up to 3 nm after thermal oxidation at 1000 °C for 30 min. However B atoms readily segregate on the surface oxide layers during thermal oxidation and became electrically inactive.¹⁹ The decrease in the electrical active B concentration by thermal oxidation made it nearly impossible to detect the electronic transition of B in SiNWs by IR-SR. The diameter of SiNWs also can be decreased by decreasing the growth temperature and the content of Ni catalyst.²⁸ These methods can be used to

prevent B segregation, but at the same time they decrease B concentration, making it difficult to detect the electronic transitions of B in SiNWs. Hence, characterization of the electronic transitions of B in SiNWs with lower diameters remains problematic.

The H passivation effect is a well-known phenomenon in Si. Hydrogen atoms migrate to the bond center site between B and Si atoms, resulting in the formation of H-B passivation centers in B-doped Si. The formation of these H-B passivation centers reduces the symmetry of B atoms from the tetrahedral (T_d) symmetry of substitutional B atoms to axial symmetry with respect to the H-B axis, which in turn causes a splitting of the triply-degenerate B mode with T_d point-group symmetry into a doublet plus a singlet with C_{3v} point group symmetry, as shown in Fig. 6c. This structural change can be used to assign the peak at 625 cm^{-1} . The results of IR-SR measurements before and after hydrogenation at 180 °C for 30 min are shown in Figure 6a. After hydrogenation, a peak was newly observed at about 669 cm^{-1} . This is the same pattern as seen in the results of the Raman measurements shown in Fig. 6b. The newly observed Raman peak at 650 - 680 cm^{-1} after hydrogenation is due to the

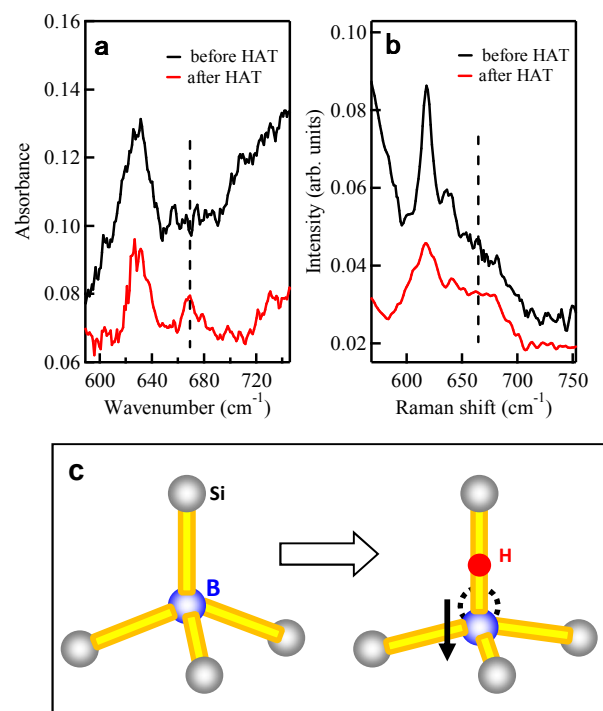


Fig. 6 (a) IR-SR absorption spectra and (b) Raman spectra observed for B-doped SiNWs synthesized using $\text{Si}_{189}\text{Ni}_1\text{B}_{10}$ targets before and after hydrogenation at 180 °C for 30 min. (c) Illustration of the formation of an H-B passivation center. The dotted circle shows the initial B position before hydrogenation. B-doped SiNWs were synthesized using $\text{Si}_{189}\text{Ni}_1\text{B}_{10}$ targets.

B local vibrational mode being perturbed by the formation of H-B passivation centers.¹⁵ Based on these results, the peak at 669 cm^{-1} after hydrogenation is assigned to the absorption peak of B in H-B passivation centers, proving again that the 625 cm^{-1} peak is due to the IR absorption peak of B in SiNWs. These results show that micro-FT-IR using the IR-SR beam is a potentially useful technique for characterizing the status of B atoms in SiNWs. The values of local vibrational modes and

electronic transitions of B in SiNWs observed by IR-SR and Raman measurements are summarized in Table 1.

Table 1. Local vibrational modes and electronic transitions of B in SiNWs observed by IR-SR and Raman scattering measurements. The values in the parentheses are for B-doped bulk Si.

	Local vibrational modes (cm ⁻¹)			Electronic transitions (cm ⁻¹)	
	¹¹ B	¹⁰ B	B in H-B	1s-2p	1s-3p
IR-SR	625	—	669	278 (278)	319 (320)
Raman	618 (619)	643 (640)	650-680 (650)		

Conclusions

In conclusion, a new peak was observed at 625 cm⁻¹ by micro-FT-IR measurements using the IR-SR beamline at SPring-8. The peak was assigned to the IR-SR absorption peak of B in SiNWs. The electronic transitions from the ground state of a neutral B acceptor atom to excited levels were also newly observed at about 278 and 319 cm⁻¹. The results for B-doped SiNWs with a diameter of 20 nm show no significant shift in impurity levels, showing that the B acceptor levels in SiNWs with a diameter of 20 nm keep the same position as that in bulk Si. The use of thinned NW samples, combined with a high-brilliance IR-SR beam, made it possible to evaluate the electronic transition of neutral B acceptor atoms in highly B-doped Si samples. This is the first observation of the electronic transition of neutral B acceptor atoms for highly B-doped Si. The hydrogen passivation effect was also investigated using IR-SR measurements. The B peak for the H-B passivation center was observed at 669 cm⁻¹. These results clearly demonstrate the clear potential usefulness of the IR-SR method as a new tool for characterizing nanomaterials.

Acknowledgements

This work was supported by JSPS KAKENHI Grant numbers 26246021 and 26600049. This work was also partly supported by the World Premier International Research Center Initiative (WPI Initiative), MEXT, Japan. The synchrotron radiation experiments were performed on the BL43IR infrared beamline at SPring-8 with the approval of the Japan Synchrotron Radiation Research Institute (JASRI) (Proposal No. 2009A1314, 2013A1153).

Notes and references

^a International Center for Materials Nanoarchitectonics, National Institute for Materials Science, 1-1 Namiki, Tsukuba, Ibaraki, 305-0044, Japan

^b Japan Synchrotron Radiation Research Institute, 1-1-1 Kôto, Sayo, Hyogo, 679-5198, Japan

Electronic Supplementary Information (ESI) available: See DOI: 10.1039/b000000x/

- 1 Y. Li, F. Qian, J. Xiang and C. M. Lieber, *Materials today*, 2006, **9**, 18.
- 2 A. I. Hochbaum and P. Yang, *Chem. Rev.* 2010, **110**, 527.
- 3 R. Rurali, *Rev. Mod. Phys.* 2010, **82**, 427.

- 4 K. Q. Peng and S. T. Lee, *Adv. Mater.* 2011, **23**, 198.
- 5 Y. Cui, X. Duan, J. Hu and C. M. Lieber, *J. Phys. Chem.* 2000, **B104**, 5213.
- 6 D. D. D. Ma, C. S. Lee and S. T. Lee, *Appl. Phys. Lett.* 2001, **79**, 2468.
- 7 K. K. Lew, L. Pan, T. E. Bogart, S. M. Dilts, E. C. Dickey, J. M. Redwing, Y. Wang, M. Cabassi, T. S. Mayer and S. W. Novak, *Appl. Phys. Lett.* 2004, **85**, 3101.
- 8 Y. Wang, K. K. Lew, T. T. Ho, L. Pan, S. W. Novak, E. C. Dickey, J. M. Redwing and T. S. Mayer, *Nano Lett.* 2005, **5**, 2139.
- 9 C. Yang, Z. Zhong and C. M. Lieber, *Science*. 2005, **310**, 1304.
- 10 M. Amato, S. Ossicini and R. Rurali, *Nano Lett.* 2011, **11**, 594.
- 11 Y. Zhao, J. T. Smith, J. Appenzeller and C. Yang, *C. Nano Lett.* 2011, **11**, 1406.
- 12 N. Fukata, M. Mitome, T. Sekiguchi, Y. Bando, M. Kirkham, J-il. Hong, Z. L. Wang and R. Snyder, *ACS NANO* 2012, **6**, 8887.
- 13 M. Amato, R. Rurali and S. Ossicini, *J. Comput. Electron.* 2012, **11**, 272.
- 14 M. Amato, R. Rurali, M. Palumbo and S. Ossicini, *J. Phys. D: Appl. Phys.* 2014, **47**, 394013.
- 15 N. Fukata, J. Chen, T. Sekiguchi, N. Okada, K. Murakami, T. Tsurui and S. Ito, *Appl. Phys. Lett.* 2006, **89**, 203109.
- 16 N. Fukata, J. Chen, T. Sekiguchi, S. Matsushita, T. Oshima, N. Uchida, K. Murakami, T. Tsurui and S. Ito, *Appl. Phys. Lett.* 2007, **90**, 153117.
- 17 N. Fukata, *Adv. Mater.* 2009, **21**, 2829.
- 18 N. Fukata, R. Takiguchi, S. Ishida, S. Yokono, S. Hishita and K. Murakami, *ACS NANO* 2012, 3278.
- 19 N. Fukata, S. Ishida, S. Yokono, R. Takiguchi, J. Chen, T. Sekiguchi and K. Murakami, *Nano Lett.* 2011, **11**, 651.
- 20 J. I. Pankove, D. E. Carlson, J. E. Berkeyheiser and R. O. Wance, *Phys. Rev. Lett.* 1983, **51**, 2224.
- 21 K. J. Chang and D. J. Chadi, *Phys. Rev. Lett.* 1988, **60**, 1422.
- 22 M. Stavola, K. Bergman, S. J. Pearton and J. Lopata, *Phys. Rev. Lett.* 1988, **61**, 2786.
- 23 P. J. H. Denteneer, C. G. Van de Walle and S. T. Pantelides, *Phys. Rev. B.* 1989, **39**, 10809.
- 24 M. Suezawa, N. Fukata, M. Saito and H. Yamada-Kaneta, *Phys. Rev. B.* 2002, **65**, 075214.
- 25 N. Fukata, S. Fukuda, S. Sato, K. Ishioka, M. Kitajima, T. Hishita and K. Murakami, *Phys. Rev. B.* 2005, **72**, 245209.
- 26 R. S. Wagner and W.C. Ellis, *Appl. Phys. Lett.* 1964, **4**, 89.
- 27 S. Piscanec, M. Cantoro, A. C. Ferrari, J. A. Zapien, Y. Lifshitz, S. T. Lee, S. Hofmann and J. Robertson, *Phys. Rev. B.* 2003, **68**, 241312(R).
- 28 N. Fukata, T. Oshima, N. Okada, T. Kizuka, T. Tsurui, S. Ito and K. Murakami, *J. Appl. Phys.* 2006, **100**, 024311.
- 29 N. Fukata, S. Sasaki, S. Fujimura, H. Haneda and K. Murakami, *Jpn. J. Appl. Phys.* 1996, **35**, 3937.
- 30 C. T. Kirk, *Phys. Rev. B.* 1988, **38**, 1255.
- 31 C. P. Herrero and M. Stutzmann, *Phys. Rev. B.* 1988, **38**, 12668.
- 32 E. Burstein, G. Picus, B. Henvis and R. Wallis, *J. Phys. Chem. Solids.* 1956, **1**, 65.
- 33 H. J. Hrostowski and R. H. J. Kaiser, *J. Phys. Chem. Solids.* 1958, **4**, 148.
- 34 B. Pajot, *J. Phys. Chem. Solids.* 1964, **25**, 613.

- 35 B. O. Kolbesen, *Appl. Phys. Lett.* 1975, **27**, 353.
- 36 S. C. Baber, *Thin Solid Films*, 1980, **72**, 201.
- 37 S. C. Jain, W. Schoenmaker, R. Lindsay, P. A. Stolk, S. Decoutere, M. Willander and H. E. Maes, *J. Appl. Phys.* 2002, **91**, 8919.
- 38 T.-L. Chan, M. L. Tiago, E. Kaxiras and J. R. Chelikowsky, *Nano Lett.* 2008, **8**, 596.
- 39 M. Diarra, Y-M. Niquet, C. Delerue and G.Allan. *Phys. Rev. B.* 2007, **75**, 045301.
- 40 M. T. Björk, H. Schmid, J. Knoch, H. Riel and W. Riess, *Nature Nanotech.* 2009, **4**, 103.